International Journal on Magnetic Particle Imaging
Vol 8, No 1, Suppl 1, Article ID 2203061, 4 Pages

Infinite Science Publishing

Proceedings Article

Comparison of Reconstruction Methods for Measured FFL Data

Jonas Schumacher[a,b,*] · Mandy Ahlborg[a,b] · Eric Aderhold[a,b] · Pascal Stagge[a,b] · Thorsten M. Buzug[a,b] · Matthias Gräser[a,b]

[a]Fraunhofer Research Institution for Individualized and Cell-Based Medical Engineering IMTE, Lübeck, Germany
[b]Institute of Medical Engineering, University of Lübeck, Lübeck, Germany
[*]Corresponding author, email: jonas.schumacher@imte.fraunhofer.de

Abstract

System matrix and x-space resonstruction are two of the main approaches for image reconstruction of field free line magnetic particle imaging. A comparative study of both options is performed on data from a phantom measurement in a permanent magnet-based scanner system. The system matrix reconstruction is performed in a hybrid fashion with data obtained in a spectrometer. This data is also used to obtain the relaxation time and particle diameter of the particles used. A deconvolution can then be used to enhance the image quality of the x-space approach which is compared to the system matrix reconstruction. A slight blurring can be depicted in the x-space reconstruction but overall a good agreement between both approaches is reached with the Structural Similarity Index yielding a value of 0.79.

I. Introduction

In field free line (FFL) magnetic particle imaging (MPI), a commonly used reconstruction scheme is the x-space method [1]. Every kind of superparamagnetic iron oxide nanoparticle (SPION) exhibits a different behaviour when imaged. The x-space method has thus been enhanced with information on the relaxation behaviour of the particles [2]. In contrast, a system matrix can be obtained calibrating the particle system and scanning setup [3]. This reference measurement contains all information on the particle behaviour within a given imaging system. Since the field of view (FOV) has to be sampled on a reasonably dense grid, the procedure is time-consuming. One method to partially overcome this limitation is using a hybrid system matrix obtained with a dedicated device [4]. With our FFL scanner based on a Halbach arrangement of permanent magnets [5], we obtained two-dimensional data of a phantom. This data is used here to compare the image quality of the two aforementioned image reconstruction approaches. A similar study has been performed by Ilbey et al. [6] on simulated data.

II. Methods and materials

The scanner used for this study features an FFL generated between two Halbach dipole cylinders which are aligned on the same axis but with opposing orientation of the permanent magnet remanences [5]. Due to the field vector being oriented along the bore, a single solenoid along the bore is used for a translation of the FFL in the orthogonal imaging plane. A mechanical rotation of the gantry then allows for the acquisition of two-dimensional data. An adjustable gradiometric receive coil combined with a four stage bandstop filter and a custom low noise amplifier (LNA) form the receive chain of the system. The spectrometer used for this study is capable of three dimensional excitation [7], but only one channel was used here for the acquisition of a hybrid system matrix.

II.I. Measurement setup

The spectrometer measurement was performed on an undiluted sample of Perimag (micromod Partikeltechnologie GmbH) with an offset field resolution of 0.5 mT and a maximum offset of 25 mT. The measurements with the scanner were performed using a custom data acquisition system [8] and controlled by a custom measurement framework[1]. The control loop for the drive field is set to an amplitude of 20 mT at a frequency of 25 kHz. The data is then processed within our Julia-based reconstruction framework.

II.II. X-space reconstruction

The basic x-space approach transfers the time-domain data into an image by applying a velocity compensation and a regridding [1]. As described in [2], the particles' response to the drive field can be approximated by the Langevin theory of paramagnetism combined with a first-order Debye process, which results in a blurred image. Thus, for a fair comparison with the hybrid system matrix-based method, two deconvolutions are added to the process. The main influences on the blurring are the particle core diameter D_k and the relaxation time constant τ. For including a deconvolution based on the particle behaviour, both parameters have to be estimated. This is achieved by fitting the model to the data obtained in the spectrometer at 0 mT offset by minimizing the sum of squared differences with the Nelder–Mead method. Since the data does not contain the fundamental frequency, this component is also removed from the modelled signal. Utilizing the estimated values, the deconvolution can be split into two parts. The signal is first deconvolved with the Debye kernel in order to get a symmetric signal. This step is important to be able to merge the two half waves of the signal without widening the PSF. The signal can then be processed with the classic x-space approach. Afterwards, the deconvolution with the derivative of the Langevin function is performed and the final image is reconstructed with an inverse Radon transform. Both deconvolutions are of the Wiener kind and have the signal-to-noise ratio set to 1.

II.III. Hybrid system matrix reconstruction

The hybrid system matrix-based reconstruction is performed by applying the Kaczmarz algorithm [9] on each of the angles individually yielding a one-dimensional projection (cf. [10]). Only two iterations are performed with $\lambda = 0.001$. These projections are then sorted into a sinogram and reconstructed into an image with an inverse Radon transform. Negative values were allowed during the Kaczmarz iterations and later set to zero in the final image for plausability reasons.

[1] https://github.com/MagneticParticleImaging/MPIMeasurements.jl

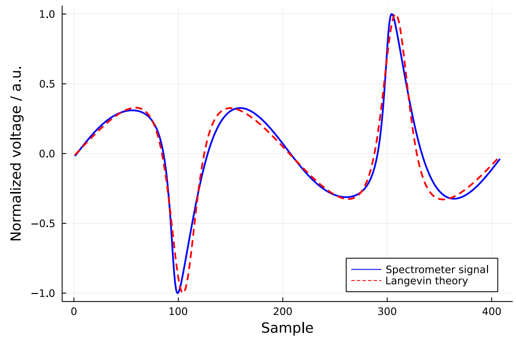

Figure 1: Comparison of the particle signal and its estimation based on the Langevin theory of paramagnetism and a first-order Debye process. The fundamental frequency is removed from the simulated signal for comparability.

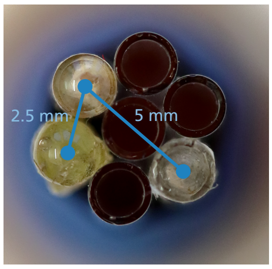

Figure 2: Front view of the phantom. The three capillaries with an inner diameter of 1.89 mm depicted by the dots were filled with undiluted Perimag and closed with glue while the remaining four stayed empty.

III. Experiments

With the acquired system matrix data, the estimation of the particle diameter yields $D_k = 15.5\,\text{nm}$ while the relaxation time constant is estimated to be $\tau = 0.17\,\mu\text{s}$. The resulting fit can be seen in Figure 1.

For the reconstruction study, the rotation frequency of the gantry was set to 1 Hz by adjusting the step motor to a speed matching the gear ratio of the bevel gear drive. After controlling the field amplitude, a measurement time of 1 s was used for acquiring projections from a phantom made of capillaries (cf. Figure 2). The data was corrected by a background measurement and a transfer function and then binned by averaging the data of one rotation by a factor of 100 into 250 periods and thus angles. In both reconstruction approaches, the number of harmonics was limited to 50.

The resulting image of the x-space reconstruction can be depicted in Figure 3 while the hybrid system matrix reconstruction is shown in Figure 4. Both images were cut to a circle to account for ring artifacts that are clearly

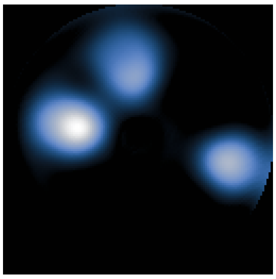

Figure 3: X-space reconstruction of the phantom. The dots show a slight blurring.

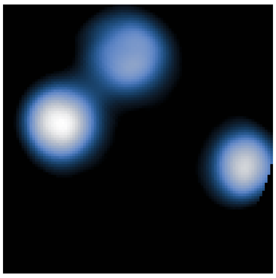

Figure 4: Hybrid system matrix reconstruction of the phantom. The dots appear more round compared to the x-space reconstruction.

out of the FOV.

A visual inspection of the x-space image shows a slight blurring of the points away from the center. In order to compare the reconstruction quantitatively, the Structural Similarity Index (SSIM) was calculated between the two reconstructed images with the aforementioned cut applied. The metric yields a value of 0.79 after matching the reconstrucion sizes with a scaling factor to account for the different pixel resolutions due to the discarding of data after the velocity compensation of the x-space reconstruction. The computation times of both approaches are negligible compared to the inverse Radon transform which is needed in both cases. Note that both reconstructions can be parallelized for each angle up to the point of yielding the sinogram.

IV. Discussion

The derived core diameter of $D_k = 15.5\,\text{nm}$ of the particles approximately agrees with the literature [11] where a core size of $D_k = 19\,\text{nm}$ was fitted from spectrometer data. For the relaxation time constant no data were found in literature. Both reconstructions yield nicely separated dots and are also quite similar according to the SSIM metric. The slight blurring towards the rim is attributed to the close proximity of the particle samples to the edge of the field. The edges generated by this fact might pose a problem for the Wiener deconvolution.

V. Conclusion

Both approaches to reconstructing the data generated by our FFL MPI scanner produce good results. The particle dynamics are most likely more accurately described by the hybrid system matrix and the dots show less blurring with this reconstruction. It can thus be concluded that the hybrid system matrix reconstruction is favourable in terms of image quality for the given scanner system and implementation of the reconstruction algorithms.

Acknowledgments

Research funding: The Fraunhofer IMTE is supported by the EU (EFRE) and the State Schleswig-Holstein, Germany (Project: IMTE – Grant: 124 20002 / LPW-E1.1.1/1536).

References

[1] P. W. Goodwill and S. M. Conolly. The x-space formulation of the magnetic particle imaging process: 1-d signal, resolution, bandwidth, snr, sar, and magnetostimulation. *IEEE Transactions on Medical Imaging*, 29(11):1851–1859, 2010, doi:10.1109/TMI.2010.2052284.

[2] L. R. Croft, P. W. Goodwill, and S. M. Conolly. Relaxation in x-space magnetic particle imaging. *IEEE Transactions on Medical Imaging*, 31(12):2335–2342, 2012, doi:10.1109/TMI.2012.2217979.

[3] B. Gleich and J. Weizenecker. Tomographic imaging using the nonlinear response of magnetic particles. *Nature*, 435(7046):1214–1217, 2005, doi:10.1038/nature03808.

[4] A. von Gladiß, M. Gräser, P. Szwargulski, T. Knopp, and T. M. Buzug. Hybrid system calibration for multidimensional magnetic particle imaging. *Physics in medicine and biology*, 62(9):3392–3406, 2017, doi:10.15480/882.1892.

[5] M. Weber, J. Beuke, A. von Gladiss, K. Gräfe, P. Vogel, V. C. Behr, and T. M. Buzug. Novel field geometry using two halbach cylinders for ffl-mpi. *International Journal on Magnetic Particle Imaging*, 4(1), 2018, doi:10.18416/IJMPI.2018.1811004.

[6] S. Ilbey, C. B. Top, A. Güngör, T. Çukur, E. U. Saritas, and H. E. Güven. Comparison of system-matrix-based and projection-based reconstructions for field free line magnetic particle imaging. *International Journal on Magnetic Particle Imaging*, 3(1), 2017.

[7] X. Chen, M. Graeser, A. Behrends, A. von Gladiss, and T. M. Buzug. First measurement and snr results of a 3d magnetic particle spectrometer. *International Journal on Magnetic Particle Imaging*, 4(1), 2018, doi:10.18416/IJMPI.2018.1810001.

[8] N. Hackelberg, J. Schumacher, M. Graeser, and T. Knopp, A flexible high-performance signal generation and digitization plattform basedon low-cost hardware, in *International Journal on Magnetic Particle Imaging - Proceedings of the International Workshop on Magnetic Particle Imaging 2022 (submitted)*, 2022.

[9] T. Knopp, P. Szwargulski, F. Griese, M. Grosser, M. Boberg, and M. Möddel. Mpireco.jl: Julia package for image reconstruction in mpi. *International Journal on Magnetic Particle Imaging*, 5(1):9 pp, 2019, doi:10.18416/ijmpi.2019.1907001.

[10] A. von Gladiss, J. Beuke, M. Weber, A. Malhotra, A. Behrends, A. Cordes, M. Stille, V. C. Behr, P. Vogel, K. Gräfe, T. Friedrich, K. Lüdtke-Buzug, A. Neumann, M. Ahlborg, and T. M. Buzug, Dynamic 2d imaging with an mpi scanner featuring a mechanically rotated ffl, in *9th International Workshop on Magnetic Particle Imaging*, 5, 2019.

[11] D. Eberbeck, C. L. Dennis, N. F. Huls, K. L. Krycka, C. Gruttner, and F. Westphal. Multicore magnetic nanoparticles for magnetic particle imaging. *IEEE Transactions on Magnetics*, 49(1):269–274, 2013, doi:10.1109/TMAG.2012.2226438.